1-1-2012

Frequency selection in absolute phase maps recovery with two frequency projection fringes

Yi Ding
Huazhong University of Science and Technology

Jiangtao Xi
University of Wollongong, jiangtao@uow.edu.au

Yanguang Yu
University of Wollongong, yanguang@uow.edu.au

Wengqing Cheng
Huazhong University of Science and Technology

Shu Wang
Huazhong University of Science and Technology

See next page for additional authors

Frequency selection in absolute phase maps recovery with two frequency projection fringes

Abstract

In a recent published work we proposed a technique to recover the absolute phase maps of two fringe patterns with different spatial frequencies. It is demonstrated that a number of selected frequency pairs can be used for the proposed approach, but the published work did not provide a guideline for frequency selection. In addition, the performance of the proposed technique in terms of its anti-noise capability is not addressed. In this paper, the rules for selecting the two frequencies are presented based on theoretical analysis of the proposed technique. Also, when the two frequencies are given, the anti-noise capability of technique is formulated and evaluated. These theoretical conclusions are verified by experimental results.

Keywords

frequency, phase, selection, maps, recovery, two, projection, fringes, absolute

Disciplines

Physical Sciences and Mathematics

Publication Details

Y. Ding, J. Xi, Y. Yu, W. Cheng, S. Wang & J. F. Chicharo, "Frequency selection in absolute phase maps recovery with two frequency projection fringes," Optics Express, vol. 20, (12) pp. 13238-13251, 2012.

Authors

Yi Ding, Jiangtao Xi, Yanguang Yu, Wengqing Cheng, Shu Wang, and Joe F. Chicharo

Frequency selection in absolute phase maps recovery with two frequency projection fringes

Yi Ding,[1,2] Jiangtao Xi,[2,*] Yanguang Yu,[2] Wenqing Cheng,[1] Shu Wang,[1] and Joe F. Chicharo[2]

[1]*Department of Electronic and Information Engineering, Huazhong University of Science and Technology, Wuhan, Hubei, 430074, China*

[2] *School of Electrical Computer and Telecommunications Engineering, University of Wollongong, Wollongong, NSW, 2522, Australia*

[*]*jiangtao@uow.edu.au*

Abstract: In a recent published work we proposed a technique to recover the absolute phase maps of two fringe patterns with different spatial frequencies. It is demonstrated that a number of selected frequency pairs can be used for the proposed approach, but the published work did not provide a guideline for frequency selection. In addition, the performance of the proposed technique in terms of its anti-noise capability is not addressed. In this paper, the rules for selecting the two frequencies are presented based on theoretical analysis of the proposed technique. Also, when the two frequencies are given, the anti-noise capability of technique is formulated and evaluated. These theoretical conclusions are verified by experimental results.

OCIS codes: (120.5050) Phase measurement; (100.2650) Fringe analysis; (100.5088) Phase unwrapping.

References and links

1. S. Zhang, X. Li, and S. T. Yau, "Multilevel quality-guided phase unwrapping algorithm for real-time three-dimensional shape reconstruction," Appl. Opt. **46**(1), 50–57 (2007).
2. J. M. Huntley and H. O. Saldner, "Temporal phase-unwrapping algorithm for automated interferogram analysis," Appl. Opt. **32**(17), 3047–3052 (1993).
3. H. Zhao, W. Chen, and Y. Tan, "Phase-unwrapping algorithm for the measurement of three-dimensional object shapes," Appl. Opt. **33**(20), 4497–4500 (1994).
4. H. J. Chen, J. Zhang, D. J. Lv, and J. Fang, "3-D shape measurement by composite pattern projection and hybrid processing," Opt. Express **15**(19), 12318–12330 (2007).
5. J. L. Li, H. J. Su, and X. Y. Su, "Two-frequency grating used in phase-measuring profilometry," Appl. Opt. **36**(1), 277–280 (1997).
6. J. Li, L. G. Hassebrook, and C. Guan, "Optimized two-frequency phase-measuring-profilometry light-sensor temporal-noise sensitivity," J. Opt. Soc. Am. A **20**(1), 106–115 (2003).
7. K. Liu, Y. Wang, D. L. Lau, Q. Hao, and L. G. Hassebrook, "Dual-frequency pattern scheme for high-speed 3-D shape measurement," Opt. Express **18**(5), 5229–5244 (2010).
8. S. Zhang, "Phase unwrapping error reduction framework for a multiple-wavelength phase-shifting algorithm," Opt. Eng. **48**(10), 105601 (2009).
9. J. M. Huntley and H. O. Saldner, "Error-reduction methods for shape measurement by temporal phase unwrapping," J. Opt. Soc. Am. A **14**(12), 3188–3196 (1997).
10. H. O. Saldner and J. M. Huntley, "Temporal phase unwrapping: application to surface profiling of discontinuous objects," Appl. Opt. **36**(13), 2770–2775 (1997).
11. S. Zhang, "Digital multiple-wavelength phase-shifting algorithm," Proc. SPIE **7432**, 74320N, 74320N-11 (2009).
12. C. E. Towers, D. P. Towers, and J. D. C. Jones, "Absolute fringe order calculation using optimisied multi-frequency selection in full-filed profilometry," Opt. Lasers Eng. **43**(7), 788–800 (2005).
13. J. C. Wyant, "Testing aspherics using two-wavelength holography," Appl. Opt. **10**(9), 2113–2118 (1971).
14. C. Polhemus, "Two-wavelength interferometry," Appl. Opt. **12**(9), 2071–2074 (1973).
15. Y.-Y. Cheng and J. C. Wyant, "Two-wavelength phase shifting interferometry," Appl. Opt. **23**(24), 4539–4543 (1984).
16. K. Creath, "Step height measurement using two-wavelength phase-shifting interferometry," Appl. Opt. **26**(14), 2810–2816 (1987).
17. K. Houairi and F. Cassaing, "Two-wavelength interferometry: extended range and accurate optical path difference analytical estimator," J. Opt. Soc. Am. A **26**(12), 2503–2511 (2009).

#164466 - $15.00 USD Received 12 Mar 2012; revised 3 May 2012; accepted 14 May 2012; published 29 May 2012

18. Y. Ding, J. Xi, Y. Yu, and J. Chicharo, "Recovering the absolute phase maps of two fringe patterns with selected frequencies," Opt. Lett. **36**(13), 2518–2520 (2011).
19. K. Liu, Y. Wang, D. L. Lau, Q. Hao, and L. G. Hassebrook, "Gamma model and its analysis for phase measuring profilometry," J. Opt. Soc. Am. A **27**(3), 553–562 (2010).
20. Y. Wang, K. Liu, Q. Hao, X. Wang, D. L. Lau, and L. G. Hassebrook, "Robust active stereo vision using Kullback-Leibler divergence," IEEE Trans. Pattern Anal. Mach. Intell. **34**(3), 548–563 (2012).

1. Introduction

Fringe projection profilometry (FPP) is one of the most promising approaches for non-contact 3D shape measurement. A challenging task associated with existing phase measurement techniques in FPP is phase unwrapping operation, which aims to recover the absolute phase maps from the wrapped phase maps falling in $(-\pi,\pi)$. Although various phase unwrapping methods have been proposed, such as spatial [1], temporal [2,3] and period coding [4], recovery of absolute phase maps is still a challenging task when the wrapped phase maps contain noise, sharp changes or discontinuities [2].

To achieve reliable and accurate phase unwrapping for FPP, a variety of temporal phase unwrapping approaches have been proposed following work of Huntley and Saldner [2]. The general idea behind the temporal method is the use of multiple fringe patterns that are projected onto the project, yielding a sequence of wrapped phase maps as a function of time *t*. These phase maps can be considered as a 3D phase map $\phi(m,n,t)$, denoting the wrapped phase value at pixel (m,n) at the *t*th phase map ($t = 0, 1, 2, \ldots, s$). Phase unwrapping can be carried out along any path in the 3D space in order to avoid noise or boundaries and thus achieving correct recovery of the absolute phase map. While the method proposed in [2] is demonstrated to be effective for accurate phase unwrapping, it also suffers from the drawback of requiring many intermediate phase patterns (e.g., 7 sets of fringe patterns were employed in [2]), which is obviously not suitable for fast or real-time measurement. In order to increase the efficiency, Zhao, *et al.* [3] proposed to use two image patterns, one of which has a very low spatial frequency in contrast to the other. In particular, the low spatial frequency pattern only has a single fringe. Such a pattern has its absolute phase value falling within the range $(-\pi,\pi)$, and hence it can be used as a reference to calculate the fringe number of the other fringe pattern, thus yielding its absolute phase map. Li, *et al.* [5,6] also employ the phase map of single fringe pattern as reference to unwrap high spatial frequency fringe patterns, and it is shown that the spatial frequency of the pattern to be unwrapped is determined by the level of noise. Following the same method in [5], Liu, *et al.* [7] project a single fringe pattern and a high frequency pattern in one shot to accelerate the speed of 3D measurement. Although these approaches work well in principle, the gap between two spatial frequencies should be restricted within a range based on the noise level or steps in the low frequency phase maps. This is because under the same lighting conditions, fringe patterns with lower frequency are more vulnerable to the influence of noise or interferences [3,6,8], and use of noisy low-frequency pattern as the reference will lead to mistakes for unwrapping the high-frequency phase maps. Therefore, the techniques proposed in [3,5,6] may not work well when the phase maps are noisy or discontinuous, and multiple intermediate image patterns are still required in order to reduce the frequency gaps among adjacent patterns. This problem is studied again by Saldner and Huntley [9,10], showing that to unwrap a phase map of frequency *f*, $\log_2 f + 1$ sets of fringe patterns are required. A similar result is also reached by Zhang [8,11], indicating that the spatial frequency can be increased by a factor of 2 between two adjacent patterns. Taking a typical FPP arrangement as an example where the image pattern has 16 fringes, 5 image patterns are still required with these approaches. Towers, *et al*. [12] propose an optimal frequency selection method to increase the unambiguous range of the measurement, showing that at least three frequencies were needed for a defined reliability in fringe number calculation. Therefore, existing temporal phase unwrapping techniques still require the use of multiple image patterns, and reduction of the number of image pattern while keeping anti-noise capability is still a challenging problem.

#164466 - $15.00 USD Received 12 Mar 2012; revised 3 May 2012; accepted 14 May 2012; published 29 May 2012

A set of technologies, which are similar by name to the above and referred to as two (or multiple wavelength) interferometry, are also proposed in the area of traditional interferometry, where use of multiple light sources with different wavelengths have shown to yield significant advantages for distance measurement [13,14]. When a monochromic light with wavelength λ is used, the measurement of a optical path difference (OPD) is suffered from ambiguity of module λ, making λ to be the so-called unambiguous OPD range (UR) for the measurement. The idea behind multiple wavelength interferometry technology is that by using multiple laser beams with different wavelengths in an interferometer, the resulting interferometric pattern is equivalent to the result of using a single laser beam in the same interferometer with a much longer wavelength, implying a significant increase in UR. If the laser beams of different wavelength λ_1 and λ_2 are used in two wavelength interferometry (TWI), an interferometric patterns can be formed with the equivalent wavelength of $\lambda_{eq} = \lambda_1\lambda_2 / |\lambda_1 - \lambda_2|$, where λ_{eq} can be made much larger than λ_1 and λ_2. With the development of digital cameras and computers, the two wavelength interferometry is considerably improved by the introduction of the phase shifting algorithm [15,16]. Houairi, *et al.* [17] present an analytical algorithm, showing that the actual UR could be much larger than the equivalent wavelength depending on the wavelengths and different sources of error.

In summary of the above, we have seen two classes of research effort. On one hand, temporal phase unwrapping techniques aim to recover the absolute phase map of fringe patters used for FPP. Due to the existence of noise, multiple intermediate fringe patterns must be used. On the other hand, the approaches of multiple wavelength interferometry aim to increase of the UR for distance measurement; they employ an equivalent fringe pattern from the use of multiple laser sources with different wavelengths in the same interferometer setup. The spatial wavelength of the equivalent pattern can be made larger than the individual laser sources, hence leading to increase of the UR for distance measurement. However, it is not guaranteed that the spatial wavelength of the equivalent pattern cover the whole image (that is, the equivalent interferometric pattern contains only a single fringe), and hence they are not yet able to solve the problem of absolute phase map recovery in FPP.

In order to remedy the phase unwrapping problem in FPP described above, the authors of this paper developed a novel approach to recover the absolute phase maps of two image patterns with selected frequencies [18]. Examples were presented to show that both of the two frequencies can be high enough for the applications of FPP. However, a number of issues are still outstanding associated with the proposed technique in [18], namely, the basic rules to select the frequencies and anti-noise capability of the proposed technique, that is, the phase error bound that ensures the correct the recovered absolute phase recovery. This paper aims to address these two important issues with the aim to provide a complete solution for the implementation of the proposed technique in [18].

This paper is organized as follows. In Section 2 we firstly present a brief review of the technique in [18], and then analyze the principle for frequency selection. In Section 3, the phase error bound is given. In Section 4, experiments are presented to validate the principle on frequency selection and the phase error bound. Section 5 concludes the paper.

2. Selection of the two frequencies

2.1 The technique proposed in [18]

With the approach proposed in [18], two fringe patterns with normalized spatial frequencies f_1 and f_2 respectively are projected onto the surface of an object, where f_1 and f_2 are positive integer numbers representing the total number of fringes on the respective patterns. Let us assume that $f_1 < f_2$ and that the intensity of two fringe patterns varies in sinusoidal manner in x-direction. We have [18]:

#164466 - $15.00 USD Received 12 Mar 2012; revised 3 May 2012; accepted 14 May 2012; published 29 May 2012

$$\begin{cases} \Phi_1(x) = 2\pi m_1(x) + \phi_1(x) \\ \Phi_2(x) = 2\pi m_2(x) + \phi_2(x) \end{cases} \tag{1}$$

$$m_2(x) f_1 - m_1(x) f_2 = \Psi(x) \tag{2}$$

where $\Psi(x) = \left[f_2 \varphi_1(x) - f_1 \varphi_2(x) \right] / 2\pi$, $x \subset [1, T]$ which is the pixel index in the horizontal direction and T is the total number of pixels. $\Phi_1(x)$ and $\Phi_2(x)$ are the absolute phase maps to be recovered, $\phi_1(x)$ and $\phi_2(x)$ are the wrapped phase maps associated with the two fringe patterns with frequencies f_1 and f_2 respectively. As $\phi_1(x) \subset (-\pi, \pi)$ and $\phi_2(x) \subset (-\pi, \pi)$, $\Phi_1(x) \subset (-f_1\pi, f_1\pi)$ and $\Phi_2(x) \subset (-f_2\pi, f_2\pi)$, the task of phase unwrapping is to determine the two integers $m_1(x)$ and $m_2(x)$, $m_1(x) = -\lfloor f_1/2 \rfloor, ..., -1, 0, 1, ..., \lfloor f_1/2 \rfloor$ and $m_2(x) = -\lfloor f_2/2 \rfloor, ..., -1, 0, 1, ..., \lfloor f_2/2 \rfloor$, where $\lfloor x \rfloor$ denotes the operation to take the largest integer which is not bigger than x.

In the proposed technique in [18], we introduced an intermediate variable $\Phi_0(x)$, denoting the absolute phase map when $f_0 = 1$. $\Phi_0(x)$ varies from $-\pi$ to π monotonically with respect to x. $\Phi_1(x)$ and $\Phi_2(x)$ are related to $\Phi_0(x)$ as follows:

$$\Phi_1(x) = f_1 \Phi_0(x), \Phi_2(x) = f_2 \Phi_0(x) \tag{3}$$

The relations between $\Phi_0(x)$ and $m_1(x)$, $m_2(x)$ are displayed in Eq. (4)-(5).

$$m_1(x) = \begin{cases} \lfloor f_1/2 \rfloor & [f_1 - (f_1 \bmod 2 + 1)]\pi / f_1 \le \Phi_0(x) < \pi \\ \quad ... & \quad ... \\ \quad 1 & \pi / f_1 \le \Phi_0(x) < 3\pi / f_1 \\ \quad 0 & -\pi / f_1 < \Phi_0(x) < \pi / f_1 \\ \quad -1 & -3\pi / f_1 < \Phi_0(x) \le -\pi / f_1 \\ \quad ... & \quad ... \\ -\lfloor f_1/2 \rfloor & -\pi <_1 \Phi_0(x) \le -[f_1 - (f_1 \bmod 2 + 1)]\pi / f_1 \end{cases} \tag{4a}$$

$$m_2(x) = \begin{cases} \lfloor f_2/2 \rfloor & [f_2 - (f_2 \bmod 2 + 1)]\pi / f_2 \le \Phi_0(x) < \pi \\ \quad ... & \quad ... \\ \quad 1 & \pi / f_2 \le \Phi_0(x) < 3\pi / f_2 \\ \quad 0 & -\pi / f_2 < \Phi_0(x) < \pi / f_2 \\ \quad -1 & -3\pi / f_2 < \Phi_0(x) \le -\pi / f_2 \\ \quad ... & \quad ... \\ -\lfloor f_2/2 \rfloor & -\pi < \Phi_0(x) \le -[f_2 - (f_2 \bmod 2 + 1)]\pi / f_2 \end{cases} \tag{4b}$$

Equation (4a) and (4b) give all the possible combinations of $(m_1(x), m_2(x))$ when x varies from 1 to T. With selection of f_1 and f_2, $m_2(x) f_1 - m_1(x) f_2$ will be integer which will enable us to have a unique map relationship between $\Psi(x)$ and a pair $(m_1(x), m_2(x))$ [18]. Therefore, for a given x, we will have the value of $\Psi(x)$, and then the two absolute phases can be recovered by Eq. (1), where $(m_1(x), m_2(x))$ can be determined by minimizing the following with respect to all the possible pair of $(m_1(x), m_2(x))$ as defined by Eq. (4a) and (4b):

#164466 - $15.00 USD Received 12 Mar 2012; revised 3 May 2012; accepted 14 May 2012; published 29 May 2012

$$\underset{m_1(x),m_2(x)}{Min}\left\{\left|m_2(x)f_1 - m_1(x)f_2 - \Phi(x)\right|\right\} \tag{5}$$

The operational principle of the proposed technique can also be explained graphically using an example where $f_1 = 5$ and $f_2 = 8$. Figure 1 shows the relationship among three absolute phase maps $\Phi_0(x)$, $\Phi_1(x)$ and $\Phi_2(x)$. Figure 2 show how $\phi_1(x)$ and $\phi_2(x)$ varies over x, and Fig. 3 show how $\Psi(x)$ changes with x. It is seem that $\Psi(x)$ only takes integer values, and it switches its value when either of $\phi_1(x)$ and $\phi_2(x)$ experiences a sudden change due to the phase wrapping. It is seen that as long as all the steps in $\Psi(x)$ exhibits different height, ($m_1(x)$, $m_2(x)$) can be determined and hence $\Phi_1(x)$ and $\Phi_2(x)$ can be recovered.

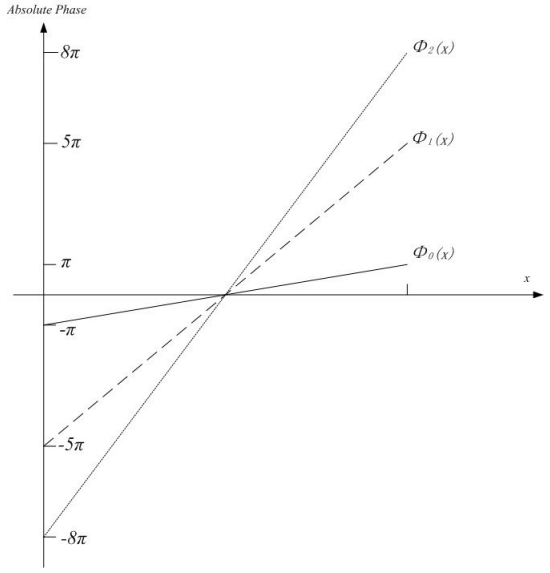

Fig. 1. Absolute phases on reference pattern image.

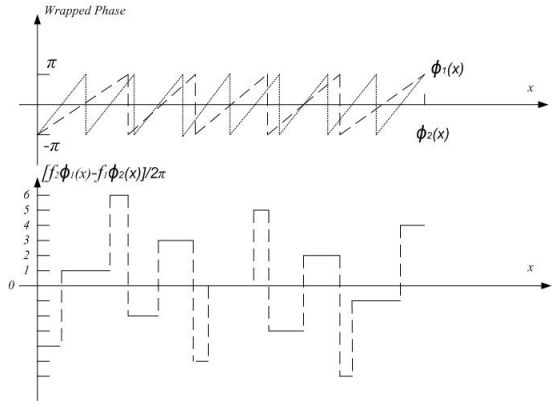

Fig. 2. Corresponding relationship between wrapped phase maps and $\Psi(x)$.

#164466 - $15.00 USD Received 12 Mar 2012; revised 3 May 2012; accepted 14 May 2012; published 29 May 2012

2.2 Principle of frequency pair selection

The validity of the approach proposed in [18] relies on the existence of unique mapping from $[f_2\phi_1(x)-f_1\phi_2(x)]/2\pi$ to a pair of $m_1(x)$ and $m_2(x)$. That is, f_1 and f_2 must be selected so that such a unique mapping relationship is held.

In order to achieve the above, let us firstly look at the relationship between $\Phi_0(x)$ and $\left(m_1(x),m_2(x)\right)$. From Eq. (4), the range of $\Phi_0(x)$ can be divided into $N_1=2\lfloor f_1/2\rfloor+1$ intervals, and the values of $\Phi_0(x)$ on interval boundaries are $(2n_1+1)\pi/f_1$ where $-\lfloor f_1/2\rfloor<n_1<\lfloor f_1/2\rfloor$. On each of the intervals $m_1(x)$ takes a different value. Similarly, Eq. (5) shows that the range of $\Phi_0(x)$ can also be divided into $N_2=2\lfloor f_2/2\rfloor+1$ intervals, the values of $\Phi_0(x)$ on interval boundaries are $(2n_2+1)\pi/f_2$ where $-\lfloor f_2/2\rfloor<n_2<\lfloor f_2/2\rfloor$. On each of the intervals $m_2(x)$ takes a different value.

When f_1 and f_2 are coprime, it is easy to show that $(2n_1+1)\pi/f_1\neq(2n_2+1)\pi/f_2$ (f_1 and f_2 will not be coprime otherwise). Hence we can say that the interval boundaries of the two types of intervals will not coincide. These two types of boundaries together can divide the range of $\Phi_0(x)$ into N intervals:

$$N=N_1+N_2-1=2\lfloor f_1/2\rfloor+2\lfloor f_2/2\rfloor+1 \tag{6}$$

Each of the intervals must correspond to an unique pair $\left(m_1(x),m_2(x)\right)$. As $\Phi_0(x)$ varies from $-\pi$ to π monotonically, these intervals on $\Phi_0(x)$ will correspond to the same number of intervals on x, denoted by $\Omega_1,\Omega_2,...,\Omega_N$. Obviously, each of $\Omega_1,\Omega_2,...,\Omega_N$ will also correspond to a unique pair $\left(m_1(x),m_2(x)\right)$. In summary of the above, we have the following:

Statement 1: If f_1 and f_2 are selected to be coprime, both of the two phase maps can be divided into strips based on the intervals $x\subset\left[\Omega_1,\Omega_2,...,\Omega_N\right]$. Each of the strips on the phase maps corresponds to a unique pair $\left(m_1(x),m_2(x)\right)$, which can be used to recover the absolute phases.

The above statement shows when f_1 and f_2 to be coprime, there exists a unique solution for the phase unwrapping problem. In order to show that the proposed approach in [18] is sufficient to work out the solution, we should also have the following:

Statement 2: When f_1 and f_2 is coprime, for any two different intervals $x_a\subset\Omega_p$, $x_b\subset\Omega_q$ *and* $p\neq q$,we must have two corresponding pairs of $\left(m_1(x),m_2(x)\right)$ based on Statement 1, which also meet the following:

$$\frac{f_2\phi_1(x_a)-f_1\phi_2(x_a)}{2\pi}\neq\frac{f_2\phi_1(x_b)-f_1\phi_2(x_b)}{2\pi}\ \text{or}\ m_2(x_a)f_1-m_1(x_a)f_2\neq m_2(x_b)f_1-m_1(x_b)f_2$$

In other words, there exists a unique mapping from $\left(m_1(x),m_2(x)\right)$ to $\frac{f_2\phi_1(x)-f_1\phi_2(x)}{2\pi}$ (that is, $m_2(x)f_1-m_1(x)f_2$).

We prove the Statement 2 by reductio ad absurdam. There are three possible scenarios making the two pairs of $\left(m_1(x),m_2(x)\right)$ different: (a) $m_1(x_a)\neq m_1(x_b)$ and $m_2(x_a)\neq m_2(x_b)$, (b) $m_1(x_a)\neq m_1(x_b)$ and $m_2(x_a)=m_2(x_b)$, and (c) $m_1(x_a)=m_1(x_b)$ and $m_2(x_a)\neq m_2(x_b)$.

#164466 - $15.00 USD Received 12 Mar 2012; revised 3 May 2012; accepted 14 May 2012; published 29 May 2012

Without loss of generality let us discuss the first case where $m_1(x_a) \neq m_1(x_b)$ and $m_2(x_a) \neq m_2(x_b)$. Assume that the following is valid:

$$m_2(x_a) f_1 - m_1(x_a) f_2 = m_2(x_b) f_1 - m_1(x_b) f_2 \tag{7}$$

Equation (7) can be rewritten as:

$$\frac{m_1(x_a) - m_1(x_b)}{m_2(x_a) - m_2(x_b)} = \frac{f_1}{f_2} \tag{8}$$

As f_1 and f_2 are coprime, Eq. (8) must be equivalent to the following:

$$m_1(x_a) - m_1(x_b) = kf_1 \text{ and } m_2(x_a) - m_2(x_b) = kf_2 \tag{9}$$

where k is an integer and $k \neq 0$.

Considering the ranges of $m_1(x)$ and $m_2(x)$ given above, we have $-\left\lfloor \frac{f_1}{2} \right\rfloor \leq m_1(x_a) \leq \left\lfloor \frac{f_1}{2} \right\rfloor$, $-\left\lfloor \frac{f_1}{2} \right\rfloor \leq m_1(x_b) \leq \left\lfloor \frac{f_1}{2} \right\rfloor$, $-\left\lfloor \frac{f_2}{2} \right\rfloor \leq m_2(x_a) \leq \left\lfloor \frac{f_2}{2} \right\rfloor$ and $-\left\lfloor \frac{f_2}{2} \right\rfloor \leq m_2(x_b) \leq \left\lfloor \frac{f_2}{2} \right\rfloor$, so:

$$-2\left\lfloor \frac{f_1}{2} \right\rfloor \leq m_1(x_a) - m_1(x_b) \leq 2\left\lfloor \frac{f_1}{2} \right\rfloor \text{and} -2\left\lfloor \frac{f_2}{2} \right\rfloor \leq m_2(x_a) - m_2(x_b) \leq 2\left\lfloor \frac{f_2}{2} \right\rfloor \tag{10}$$

Comparing Eq. (9) with Eq. (10), it is obvious that $k = \pm 1$. Hence we have

$$m_1(x_a) - m_1(x_b) = \pm f_1, m_2(x_a) - m_2(x_b) = \pm f_2 \tag{11}$$

Looking at Eq. (10) again, when Eq. (11) is held, we must have:

$$\left\lfloor \frac{f_1}{2} \right\rfloor = \frac{f_1}{2} \text{ and } \left\lfloor \frac{f_2}{2} \right\rfloor = \frac{f_2}{2} \tag{12}$$

Equation (12) implies that f_1 and f_2 are both even numbers, which is contradict to the fact that f_1 and f_2 are coprime. Hence Eq. (7) will not be true for the case (a) $m_1(x_a) \neq m_1(x_b)$ and $m_2(x_a) \neq m_2(x_b)$, thus we have the following and also Statement 2:

$$m_2(x_a) f_1 - m_1(x_a) f_2 \neq m_2(x_b) f_1 - m_1(x_b) f_2 \tag{13}$$

For the case (b) $m_1(x_a) \neq m_1(x_b)$ and $m_2(x_a) = m_2(x_b)$, and (c) $m_1(x_a) = m_1(x_b)$ and $m_2(x_a) \neq m_2(x_b)$, it is obvious that Eq. (13) will be held.

Combining Statements 1 and 2, we are able to propose the following for selection of the two frequencies f_1 and f_2 for the technique proposed in [18]:

Statement 3: If f_1 and f_2 are coprime, there existing a unique mapping from $\Psi(x)$ (that is, $[f_2\phi_1(x) - f_1\phi_2(x)]/2\pi$ *) to* $(m_1(x), m_2(x))$, which will enable us to determine $(m_1(x), m_2(x))$ in order to recover the two absolute phases using the technique proposed in [18].

3. Phase error bound

In the proposed technique [18], after calculating $[f_2\phi_1(x) - f_1\phi_2(x)]/2\pi$, we need to round the calculated $m_2(x) f_1 - m_1(x) f_2$ to the closest integer, then using Eq. (5) to find the corresponding $m_1(x)$ and $m_2(x)$. However, when $\phi_1(x)$ and $\phi_2(x)$ is corrupted by unwanted

#164466 - $15.00 USD Received 12 Mar 2012; revised 3 May 2012; accepted 14 May 2012; published 29 May 2012

noises or distortion, $[f_2\phi_1(x)-f_1\phi_2(x)]/2\pi$ may be rounded to a wrong value of $m_2(x)f_1-m_1(x)f_2$, resulting in errors in the recovered absolute phase maps. In this section we will study the performance of the proposed technique in [16] in terms of its anti-error capability.

The anti-error capability of the proposed technique depends on the gaps between any two possible values of $[f_2\phi_1(x)-f_1\phi_2(x)]/2\pi$. The larger the gap, the more unlikely the error will occur due to the rounding operation. Hence we need to find out the smallest gap between two values of $[f_2\phi_1(x)-f_1\phi_2(x)]/2\pi$, and we should also work out the relationship between the phase error in ($\phi_1(x)$, $\phi_2(x)$) and the smallest gap, which will yield the anti-noise capability of the technique in [16].

The smallest gap can be determined by the range of $[f_2\phi_1(x)-f_1\phi_2(x)]/2\pi$ and the number of gaps. As indicated by Eq. (2), we can evaluate $m_2(x)f_1-m_1(x)f_2$ to work out the range of $[f_2\phi_1(x)-f_1\phi_2(x)]/2\pi$. In order to figure out the range of $m_2(x)f_1-m_1(x)f_2$, we need to know all the possible pairs of $m_1(x)$ and $m_2(x)$.

As shown by Eq. (4) and Eq. (5), for a particular value of $m_1(x)$, $\Phi_0(x)$ spans over a range of $2\pi/f_1$, and similarly for a particular value of $m_2(x)$, $\Phi_0(x)$ cover a range of $2\pi/f_2$. When $f_1<f_2$, the $\Phi_0(x)$ associated with a particular $m_1(x)$ will span two or more intervals of $\Phi_0(x)$ with respect to different $m_2(x)$ values. Also for a given $m_1(x)$ ($m_1(x)\geq 1$), the largest value of $m_2(x)f_1-m_1(x)f_2$ corresponds to the case when $m_2(x)$ takes the largest possible value.

For a given $m_1(x)$, $\Phi_0(x)$ falls in $[2\pi m_1(x)/f_1-\pi/f_1, 2\pi m_1(x)/f_1+\pi/f_1)$. Within the same range of $\Phi_0(x)$, the largest possible $m_2(x)$ can be obtained as follows:

$$m_{2\max}(x)=\left\lceil \frac{\Phi_{0\max}(x)-\pi/f_2}{2\pi/f_2} \right\rceil \leq \frac{\Phi_{0\max}(x)-\pi/f_2}{2\pi/f_2}+1 \tag{14}$$

where $\Phi_{0\max}(x)=2\pi m_1(x)/f_1+\pi/f_1$, is the upper bound of $\Phi_0(x)$ for the given $m_1(x)$. Based on the above, the largest $m_2(x)f_1-m_1(x)f_2$ for the given $m_1(x)$ is bounded by:

$$m_2(x)f_1-m_1(x)f_2 \leq m_{2\max}(x)f_1-m_1(x)f_2 \tag{15}$$

According to Eq. (14), we have:

$$m_{2\max}(x)f_1-m_1(x)f_2 \leq (\frac{\Phi_{0\max}(x)-\pi/f_2}{2\pi/f_2})f_1-m_1(x)f_2=\frac{f_1+f_2}{2} \tag{16}$$

So we have the upper bound of $m_2(x)f_1-m_1(x)f_2$ for a given $m_1(x)$ as follows:

$$m_2(x)f_1-m_1(x)f_2 \leq \frac{f_1+f_2}{2} \tag{17}$$

Similarly, we can obtain the minimal value of $m_2(x)$ for a given $m_1(x)$ as follows:

$$m_{2\min}(x)=\left\lceil \frac{\Phi_{0\min}(x)-\pi/f_2}{2\pi/f_2} \right\rceil \geq \frac{\Phi_{0\min}(x)-\pi/f_2}{2\pi/f_2} \tag{18}$$

where $\Phi_{0\min}(x)=2\pi m_1(x)/f_1-\pi/f_1$, which is the lower bound of $\Phi_0(x)$ for the given $m_1(x)$. Based on above, the smallest $m_2(x)f_1-m_1(x)f_2$ for the given $m_1(x)$ is:

#164466 - $15.00 USD Received 12 Mar 2012; revised 3 May 2012; accepted 14 May 2012; published 29 May 2012

$$m_2(x)f_1 - m_1(x)f_2 \geq f_1 m_{2\min}(x) - f_2 m_1(x) \tag{19}$$

According to Eq. (18), we have:

$$f_1 m_{2\min}(x) - f_2 m_1(x) \geq (\frac{\Phi_{0\min}(x) - \pi / f_2}{2\pi / f_2}) f_1 - m_1(x) f_2 = -\frac{f_1 + f_2}{2} \tag{20}$$

So we have the lower bound of $m_2(x)f_1 - m_1(x)f_2$ for a given $m_1(x)$ as follows:

$$m_2(x)f_1 - m_1(x)f_2 \geq -\frac{f_1 + f_2}{2} \tag{21}$$

Combining Eq. (17) and Eq. (21) we have:

$$-\frac{f_1 + f_2}{2} \leq m_2(x)f_1 - f_2 m_1(x) \leq \frac{f_1 + f_2}{2} \tag{22}$$

From Eq. (2) and Eq. (22) we have:

$$-\frac{f_1 + f_2}{2} \leq \frac{f_2\phi_1(x) - f_1\phi_2(x)}{2\pi} \leq \frac{f_1 + f_2}{2} \tag{23}$$

The number of value gaps is determined by the number of different values in $[f_2\phi_1(x) - f_1\phi_2(x)]/2\pi$. By Eq. (6) and Statement 3, when f_1 and f_2 are coprime, the number of values in $[f_2\phi_1(x) - f_1\phi_2(x)]/2\pi$ is:

$$N = 2\lfloor f_1/2 \rfloor + 2\lfloor f_2/2 \rfloor + 1$$

So the number of value gaps is:

$$N - 1 = 2\lfloor f_1/2 \rfloor + 2\lfloor f_2/2 \rfloor \tag{24}$$

From Eq. (23) and Eq. (24), the average value gap of $[f_2\phi_1(x) - f_1\phi_2(x)]/2\pi$ is obtained as follows:

$$G = \frac{f_1 + f_2}{2\lfloor f_1/2 \rfloor + 2\lfloor f_2/2 \rfloor} < 2 \tag{25}$$

Since the values of $[f_2\phi_1(x) - f_1\phi_2(x)]/2\pi$ are integers, the minimal value gap between the values of $[f_2\phi_1(x) - f_1\phi_2(x)]/2\pi$ is 1.

If an error in $[f_2\phi_1(x) - f_1\phi_2(x)]/2\pi$ exceeds 0.5, an error will occur when rounding $[f_2\phi_1(x) - f_1\phi_2(x)]/2\pi$ into an integer. In other words, error in $[f_2\phi_1(x) - f_1\phi_2(x)]/2\pi$ must not exceed 0.5 if we want to round $[f_2\phi_1(x) - f_1\phi_2(x)]/2\pi$ into a correct integer. Assuming phase errors in the wrapped phase maps $\phi_1(x)$ and $\phi_2(x)$ are $\Delta\phi_1(x)$ and $\Delta\phi_2(x)$ respectively, we have:

$$\left| \frac{f_2\Delta\phi_1(x) - f_1\Delta\phi_2(x)}{2\pi} \right| < 0.5 \tag{26}$$

Let $\Delta\phi_{\max} = \max(|\Delta\phi_1(x)|, |\Delta\phi_2(x)|)$, from Eq. (26) we can find the upper bound of the allowable phase error:

$$0 \leq \Delta\phi_{\max} < \frac{\pi}{f_1 + f_2} \tag{27}$$

#164466 - $15.00 USD Received 12 Mar 2012; revised 3 May 2012; accepted 14 May 2012; published 29 May 2012

The above gives the upper bound of $\Delta\phi_{\max}(x)$ with which the absolute phase maps can be correctly recovered. In other words, if $\Delta\phi_{\max}(x)$ is given, we should select the two frequencies to meeting the following:

$$f_1 + f_2 < \frac{\pi}{\Delta\phi_{\max}} \tag{28}$$

If maximal phase error $\Delta\phi_{\max}(x)$ is larger than $\frac{\pi}{f_1 + f_2}$, mistakes will occur in determining the correct ($m_1(x)$, $m_2(x)$). The phase error $\Delta\phi_1(x)$ and $\Delta\phi_2(x)$ are mainly resulted from the noise (uncertainty) and non-linear distortion of the fringe pattern projection and capture system. According to the theoretical analysis and experiment results given in [19,20], phase error can be reduced by increasing the number of steps of PSP. Hence in practice we can make $0 \le \Delta\phi_1(x) < \frac{\pi}{f_1 + f_2}$ and $0 \le \Delta\phi_2(x) < \frac{\pi}{f_1 + f_2}$ in order to determine ($m_1(x)$, $m_2(x)$) correctly using the approach in [18].

4. Experiment

In order to validate the proposed rules for frequency selection, experiments have been carried out on absolute phase maps recovery for two frequencies $f_1 = 8$ and $f_2 = 15$. The camera in the experiment is DuncanTech MS3100 high resolution 3CCD camera, the projector is Hitachi CP-X260 Multimedia LCD Projector. Fringe patterns with $f_1 = 8$ and $f_2 = 15$ are projected onto a plaster hand model as the object, and the deformed fringe patterns are shown in Fig. 3 (a) and 3(b). The vertical (*y*-direction) resolution of pattern image is 1392, the horizontal (*x*-direction) is 1038.

#164466 - $15.00 USD Received 12 Mar 2012; revised 3 May 2012; accepted 14 May 2012; published 29 May 2012

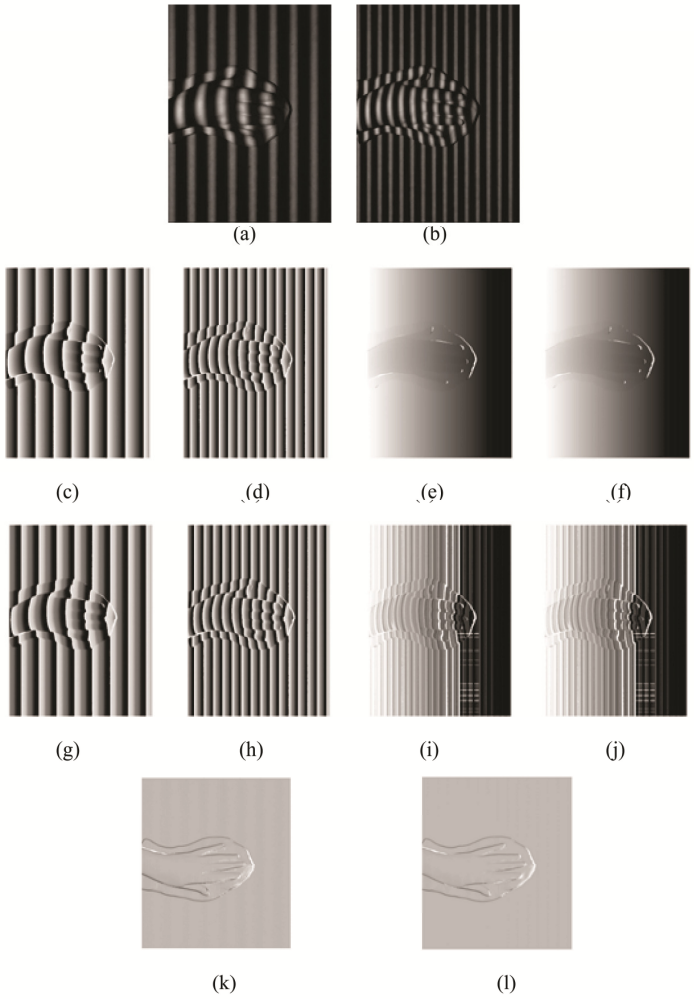

Fig. 3. Experiment results when $f_1 = 8$ and $f_2 = 15$. (a) and (b) are the deformed fringe patterns; (c) and (d) are the wrapped phase maps obtained by six-step PSP; (e) and (f) are the recovered absolute phase maps of (c) and (d); (g) and (h) are the wrapped phase maps obtained by three-step PSP; (i) and (j) are the recovered phase of (g) and (h); (k) and (l) are the three dimensional reconstruction results obtained from (e) and (f) respectively.

We firstly used the six-step Phase Shifting Profilometry (PSP) to obtain the wrapped phase maps, which are depicted in Fig. 3 (c) and 3(d). By measuring Fig. 3 (c) and 3(d) we found that $\Delta\phi_{\max}$ is about $\pi/100$ in this experiment. Since f_1 and f_2 are coprime, $f_1 + f_2 = 23 < 100$, the requirements of Statement 3 and Eq. (27) are met and hence the absolute phase maps can be recovered from the wrapped ones, as shown by Fig. 3(e) and 3(f). Also, the results for three dimensional reconstruction in Fig. 3(k) and 3(l) also demonstrate that the proposed algorithm is able to recover the absolute phase maps.

Then we obtained another set of wrapped phase maps in Fig. 3(g) and 3(h). As we did not apply any correction and calibration, the wrapped phase maps are corrupted by nonlinear distortion with $\Delta\phi_{\max}$ being about $\pi/10$. In this case, $f_1 + f_2 = 23 > 10$, according to Eq. (27), error will occur in absolute phase maps recovery, which is confirmed by Fig. 3(g) and 3(j).

#164466 - $15.00 USD Received 12 Mar 2012; revised 3 May 2012; accepted 14 May 2012; published 29 May 2012

The above can be further confirmed looking at the recovered absolute phases on a section for y = 800. The results are shown in Fig. 4 which clearly demonstrates that absolute phases can be recovered from the wrapped ones obtained by six-step PSP, and that errors occur for the recovery of the phase maps obtained from three-step PSP.

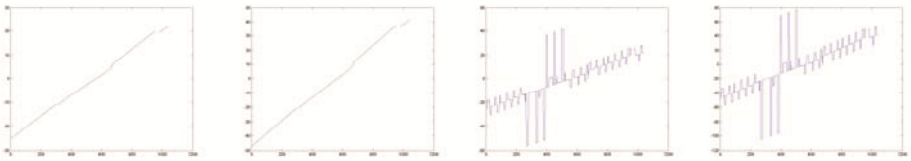

Fig. 4. Recovered absolute phases on section y = 800, the section across the palm model. (a) and (b) are the recovered absolute phases on section y = 800 for Fig. 3(e) and 3(f) by six-step PSP; (c) and (d) are the recovered phases on section y = 800 for Fig. 3(i) and 3(j) by three-step PSP.

We also carried out experiments to validate the effectiveness of our proposed rules for the object surface with steps. The object is a plane with a step of 72mm high. Fringe patterns with $f_1 = 8$ and $f_2 = 15$ are projected onto the object and the deformed fringe patterns are shown in Fig. 4(a) and 4(b). The resolution of image pattern is the same as Fig. 3, and the horizontal length of the image is 315mm. The distance between the camera and reference plane is 1200mm, the distance between the camera and projector is 300mm.

We found that the average phase jumping on section x = 240 is 5.75, so the average step height is obtained as 72.28mm. The average phase different on section x = 120 is 5.76, and so the average step height is 71.96mm. This result shows that our proposed technique can also determine the absolute phase maps when the objects are with steps.

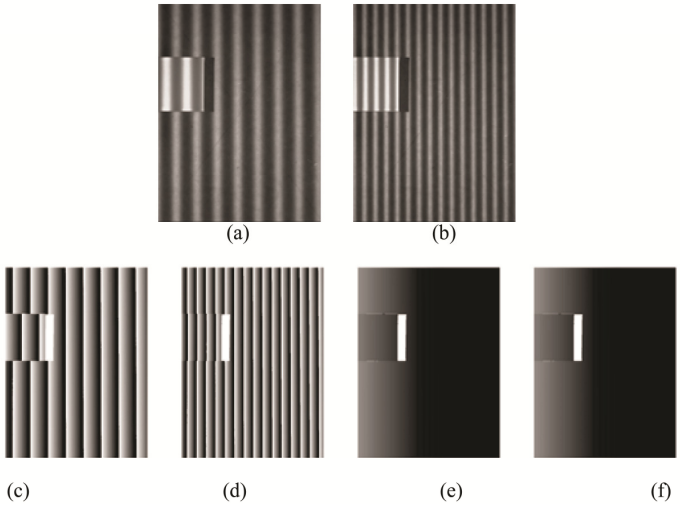

Fig. 5. Experiment on the plane with step. (a) and (b) are deformed fringe patterns; (c) and (d) are the wrapped phase maps by six-step PSP (white part are areas covered by object shadows); (e) and (f) are the absolute phase maps recovered by (c) and (d).

In order to compare with the existing two-frequency temporal phase unwrapping algorithms, we also implemented the phase unwrapping technique in Eq. (37) in [6]. Under the same experimental conditions, one of the fringe patterns has the unit frequency (i.e., only one fringe on the pattern), and the other has the spatial frequency 15. These two fringe patterns are projected onto the same plaster hand model, and the phase maps are obtained by six-step PSP algorithm. The experiment results are depicted in Fig. 6 and Fig. 7 gives the

#164466 - $15.00 USD Received 12 Mar 2012; revised 3 May 2012; accepted 14 May 2012; published 29 May 2012

absolute phase map on section $y = 800$ of the Fig. 6(e). Comparing the recovered phase map in Fig. 6 (e) with Fig. 3(e) and 3(f), it is clear that errors are observed in Fig. 6 (e) and Fig. 7. By looking at Fig. 6 (a), we find that the maximal phase error of phase map on unit frequency is about $\pi/15$, which is bigger than $\pi/16$, the threshold set Eq. (27) for correct absolute phase recovery. Note that such a large phase error is reasonable as the lower the frequency, the higher the phase noise [3,8], and such a large phase error in the wrapped unit frequency phase map has led to miscounting of the fringe orders and errors in absolute phase recovery. Looking into the results in Fig. 3 again, use of frequencies 8 and 15 enjoys the maximal phase error $\pi/100$, and hence meets the requirement of Eq. (29), thus enabling correct phase recovery by means of the proposed technique in [18].

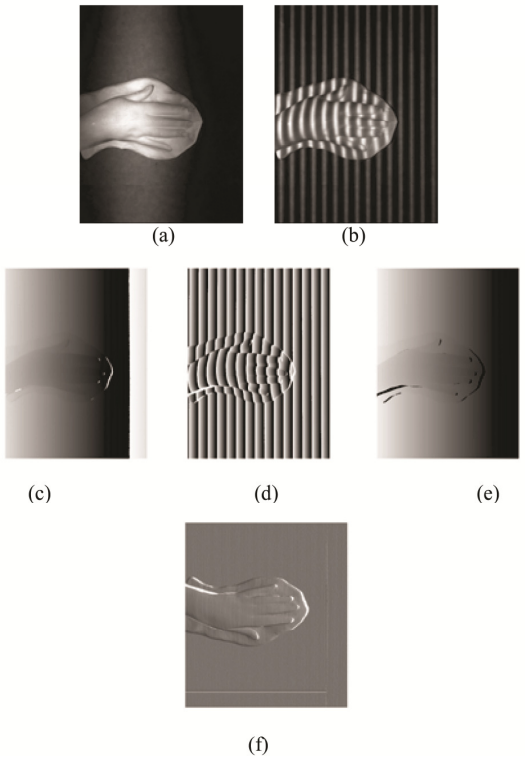

Fig. 6. Experiment by the existing algorithm. (a) and (b) are deformed fringe patterns of $f_1 = 1$ and $f_2 = 15$; (c) and (d) are the wrapped phase maps of $f_1 = 1$ and $f_2 = 15$ by six-step PSP; (e) is the absolute phase maps recovered by (c) and (d) based on the existing algorithm. (f) is the three dimensional reconstruction cloud.

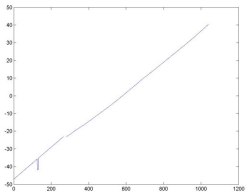

Fig. 7. Recovered absolute phase on section $y = 800$ of $f_2 = 15$ based on existing algorithm in [6].

#164466 - $15.00 USD Received 12 Mar 2012; revised 3 May 2012; accepted 14 May 2012; published 29 May 2012

5. Conclusion

We presented a guideline to select the frequencies of the two fringe patterns using the proposed technique in [18]. It is shown that when the two frequencies are coprime, the technique in [18] can be employed to recover the absolute phase maps. The anti-error ability of the proposed technique in [18] has also been investigated. We have shown that when the two frequencies f_1 and f_2 are given, the maximal allowable phase error is $\pi/(f_1+f_2)$ for accurate phase map recovery. In other words, if we know the maximal phase error $\Delta\phi_{\max}$, f_1 and f_2 should be selected in such a way that $f_1+f_2<\frac{\pi}{\Delta\phi_{\max}}$. These guidelines have been confirmed by experiments. With the guidelines presented in this paper, we are able to select the two frequencies and implement the proposed technique in [18] for various applications.

#164466 - $15.00 USD Received 12 Mar 2012; revised 3 May 2012; accepted 14 May 2012; published 29 May 2012